External Bone Size Is a Key Determinant of Strength-Decline Trajectories of Aging Male Radii[1]

Erin M R Bigelow,[1] Daniella M Patton,[1,2] Ferrous S Ward,[1,2] Antonio Ciarelli,[1,5] Michael Casden,[3] Andrea Clark,[1] Robert W Goulet,[1] Michael D Morris,[4] Stephen H Schlecht,[5] Gurjit Mandair,[6] Todd L Bredbenner,[7] David H Kohn,[2,6] and Karl J Jepsen[1,2]

[1]Department of Orthopaedic Surgery, University of Michigan, Ann Arbor, MI, USA

[2]Biomedical Engineering, University of Michigan, Ann Arbor, MI, USA

[3]School of Kinesiology, University of Michigan, Ann Arbor, MI, USA

[4]College of Literature, Science, and the Arts, University of Michigan, Ann Arbor, MI, USA

[5]Mechanical Engineering, University of Michigan, Ann Arbor, MI, USA

[6]Biological and Materials Sciences, School of Dentistry, University of Michigan, Ann Arbor, MI, USA

[7]Department of Mechanical and Aerospace Engineering, University of Colorado–Colorado Springs, Colorado Springs, CO, USA

[1] This is the author manuscript accepted for publication and has undergone full peer review but has not been through the copyediting, typesetting, pagination and proofreading process, which may lead to differences between this version and the Version of Record. Please cite this article as doi:10.1002/jbmr.3661

Received in original form September 24, 2018; revised form December 6, 2018, December 17, 2018; accepted December 19, 2018. Accepted manuscript online Month XX, 2019.

Address correspondence to: Karl J Jepsen, PhD, 109 Zina Pitcher Place, Room 2001 BSRB, University of Michigan, Ann Arbor, MI 48109-2200. E-mail: kjepsen@med.umich.edu

Journal of Bone and Mineral Research, Vol. XX, No. X, Month 2019, pp XXXX–XXXX
DOI: 10.1002/jbmr.3661

ABSTRACT

Given prior work showing associations between remodeling and external bone size, we tested the hypothesis that wide bones would show a greater negative correlation between whole-bone strength and age compared with narrow bones. Cadaveric male radii (n = 37 pairs, 18 to 89 years old) were evaluated biomechanically, and samples were sorted into narrow and wide subgroups using height-adjusted robustness (total area/bone length). Strength was 54% greater ($p < 0.0001$) in wide compared with narrow radii for young adults (< 40 years old). However, the greater strength of young-adult wide radii was not observed for older wide radii, as the wide ($R^2 = 0.565$, $p = 0.001$), but not narrow ($R^2 = 0.0004$, $p = 0.944$) subgroup showed a significant negative correlation between strength and age. Significant positive correlations between age and robustness ($R^2 = 0.269$, $p = 0.048$), cortical area (Ct.Ar; $R^2 = 0.356$, $p = 0.019$), and the mineral/matrix ratio (MMR; $R^2 = 0.293$, $p = 0.037$) were observed for narrow, but not wide radii (robustness: $R^2 = 0.015$, $p = 0.217$; Ct.Ar: $R^2 = 0.095$, $p = 0.245$; MMR: $R^2 = 0.086$, $p = 0.271$). Porosity increased with age for the narrow ($R^2 = 0.556$, $p = 0.001$) and wide ($R^2 = 0.321$, $p = 0.022$) subgroups. The wide subgroup ($p < 0.0001$) showed a significantly greater elevation of a new measure called the Cortical Pore Score, which quantifies the cumulative effect of pore size and location, indicating that porosity had a more deleterious effect on strength for wide compared with narrow radii. Thus, the divergent strength–age regressions implied that narrow radii maintained a low strength with aging by increasing external size and mineral content to mechanically offset increases in porosity. In contrast, the significant negative strength–age correlation for wide radii implied that the deleterious effect of greater porosity further from the centroid was not offset by changes in outer bone size or mineral content. Thus, the low strength of elderly male radii arose through different biomechanical mechanisms. Consideration of different strength–age regressions (trajectories) may inform clinical decisions on how best to treat individuals to reduce fracture risk. © 2019 American Society for Bone and Mineral Research

KEY WORDS: BONE; BIOMECHANICS; STRENGTH; BIOMECHANICAL MECHANISMS; AGING; RADII; MALE; PERIOSTEAL EXPANSION

Introduction

The decline in bone strength with aging increases the risk of fracturing[1] and compromises overall health, wellness, and independence.[2,3] Thus, reducing fragility fractures remains an important public health goal.[4] The reduced bone strength of elderly individuals arises from modeling and remodeling events that affect bone morphology, microstructure, and material properties.[5–9] Many of these structural and material changes are captured clinically as reductions in areal bone mineral density (aBMD). The age-related decline in strength varies between sexes and among ethnicities.[10–14] However, little is understood about why some individuals within the same sex and ethnicity show greater losses in bone strength than others, and whether this interindividual variation in bone strength decline is influenced by peak bone traits.

Recently, we reported that 14-year changes in femoral neck mass and structure differed significantly among midlife women, depending on baseline external bone size.[15] Women with narrow femoral necks showed small reductions in BMC, but large increases in bone area, whereas women with wide femoral necks showed large reductions in BMC, but only small compensatory increases in bone area. Similar associations between baseline bone area and age-related changes in mass and area have also been reported for men.[16] These studies, which were limited to data derived from hip DXA images, did not report the structural changes contributing to the differences in BMC loss or test whether the external-size dependent changes in BMC and area lead to different bone strength-decline trajectories. The greater loss in BMC for wide bones was consistent with prior work showing a positive association between remodeling and external bone size.[17–21] The mechanism responsible for the association between remodeling and external bone size remains unknown. However, because remodeling underlies age-related bone loss,[22,23] we postulated that increases in porosity and reductions in bone strength with aging would depend on external bone size. Herein, we tested the hypothesis that wide human long bones would show a greater negative correlation between whole-bone strength and age compared with narrow bones. We also examined morphological and material traits to identify the biomechanical

mechanisms that would explain the different strength-decline trajectories.

Materials and Methods

Samples

Unfixed cadaver radii (n = 37 pairs) from white male donors with no known medical conditions that would affect bone aging were acquired from the University of Michigan Anatomical Donations Program (Ann Arbor, MI, USA), Science Care (Phoenix, AZ, USA), and Anatomy Gifts Registry (Hanover, MD, USA). Human tissue use and handling was approved by the Institutional Biosafety Committee and declared exempt by the Institutional Review Board. The diaphysis was examined because the tubular structure allowed us to use engineering principles to derive biomechanical mechanisms underlying changes in bone strength. Left radii were assessed for cross-sectional morphology, whole-bone mechanical properties, and bone length (Le), which was measured from the distal articular surface to the proximal point of the radial head. Right radii were cut with a diamond-coated pathology saw (Exakt 312; Exakt Technologies, Oklahoma City, OK, USA) into five 5-mm thick sections immediately proximal to the midshaft to assess porosity, ash content, and composition (Raman spectroscopy). A 60-mm-long section of the right radius located distal to the midshaft was used to assess tissue-level mechanical properties. One donor had only a single radius available for testing; this radius was used to assess porosity and composition, resulting in 37 samples for composition and porosity and 36 samples for whole-bone mechanical testing.

Because handedness of the donors was unknown, the left hand was used to assess whole-bone strength, as the nondominant hand is often used clinically for diagnostic purposes and given the prevalence of right-handed individuals. The nondestructive assessment of morphology by pQCT was conducted on the left radii. Destructive tests (ashing, porosity, Raman spectroscopy, tissue-level mechanical properties) were conducted on the right radii. This strategy minimized the impact of handedness when assessing the contribution of morphology to whole-bone strength. Although bone morphology is affected by handedness,[24] it is less clear whether tissue-level material properties and composition are affected by handedness. It was not practical to

conduct all analyses on the left radii given that the destructive assays would have had to be done after the bones were fractured, which can affect many of the traits examined (eg, Raman, tissue-level mechanical properties).

Cross-sectional morphology

Cross-sectional morphology and cortical tissue-mineral density (Ct.TMD) were quantified from 2D images acquired at the midshaft of the left radii using pQCT (XCT 2000L, Stratec Medizintechnik, Pforzheim, Germany) and analyzed using ImageJ[25] and MomentMacro (Momentmacro.J; www.hopkinsmedicine.org/fae/ mmacro.htm).[26] Images were acquired at a 161-micron pixel size and thresholded to delineate bone from nonbone voxels. Morphological traits included total area (Tt.Ar), cortical area (Ct.Ar), marrow area (Ma.Ar), and the area moments of inertia about the anteroposterior (I_{AP}) and mediolateral axes (I_{ML}). Robustness (a measure of external bone size) was calculated as Tt.Ar/Le. Grayscale values were converted to Ct.TMD for each sample using calibration constants. A daily quality assurance scan confirmed that the difference between measured and calibrated density values was less than 1%.

Whole-bone mechanical properties

Left radii were loaded to failure in four-point bending in the medial (ulnar) to lateral (radial) direction (lateral quadrant in tension), which coincided with the natural curvature of the radius.[18,27] Sample rotation during testing was prevented by embedding the metaphyses in acrylic resin-filled square channels, aligning the faces of the squared-ends using a custom-machined fixture, and testing the samples between two walls that were parallel to the test fixture. The lower loading points were located at 25% and 75% of bone length, and the upper points were set at 33% and 67% of the lower span length. Bones were preloaded to 40 N, subjected to three preyield load–unload cycles of 400 N to 500 N to settle the bone into the test fixture, and then loaded to failure at 0.1 mm/s. Whole-bone mechanical properties were calculated from the load-deflection curves and adjusted for text fixture geometry[18] to generate the bending stiffness

(EI, Nm^2), maximum bending moment (Nm), postyield deflection (PYD; 1/m) , and work-to-fracture (N). Yield was defined as the point where a 10% reduction of the stiffness regression line intersected the load-deflection curve. Whole-bone strength refers to the maximum bending moment.[28] The loading protocol was validated by subjecting aluminum cylinders to the same load conditions and confirming that the derived material modulus was within 1% of textbook values.

Porosity

The age-related remodeling process that is responsible for increases in porosity varies radially within a cross-section.[23,29] The region adjacent to the endocortical surface shows large pores reflecting increased osteoclastic resorption, coalescence of adjacent pores, and little to no osteoblastic infilling.[29] In contrast, pores in the midcortical region tend to show a slight increase in size with aging, reflecting the early phase of intracortical bone loss. To address this spatial bone loss pattern, we first quantified porosity for the entire cross-section because these measures should reflect the overall increase in porosity with aging and should be related to changes in whole-bone strength. Second, we quantified porosity for the midcortical region to test if there was evidence that these pores were larger in the wide bones compared with the narrow bones. The sections used for porosity were macerated overnight in a warm, oxidative detergent solution (OxiClean, Church & Dwight Co., Trenton, NJ, USA) to remove fat and soft tissues, then rinsed and sonicated with PBS, and dried to constant weight at 37°C. The sections were scanned using a nanoCT system (nanotom-s; phoenix|x-ray, GE Sensing & Inspection Technologies, GmbH; Wunstorf, Germany) with consistent acquisition conditions (tungsten target, 0.3-mm aluminum filter, 2000-ms timing, three averages, one skip, 120 kV, 140 µA). Images were reconstructed at 6-µm voxel size using datos|x reconstruction 2.1 (phoenix|x-ray, GE Sensing & Inspection Technologies, GmbH). Three cross-sections spanning the 5-mm thick image volume were analyzed for each sample using Image-J,[25] which included contrast enhancement, thresholding (auto local threshold macro, v1.6), and stray pixel removal. Lacunae were excluded by filtering

voids less than 5 pixels in size. Voids that were 80% surrounded by bone and open to the endosteal surface were manually closed to capture as many pores associated with the remodeling process as possible (Fig. 1*A*).

The area and location (*x–y* coordinates of the geometric centroid) were determined for each pore. Derived measures for the entire cross-section included pore density (number of pores/cortical area), average pore area, and porosity (total pore area/cortical area). Overall porosity measures were averaged over the three cross-sections. The second set of porosity measures was assessed for eight 1-mm^2 circular midcortical ROIs that were located at 45-degree radial intervals relative to the anterior, posterior, medial, and lateral axes. Midcortex porosity was assessed for a single cross-section and included pores that were located fully within the ROI, thereby excluding the large pores located near the endosteum.

A new parameter called cortical pore score ($CPS_{plane} = \Sigma A_i\, d_i^2$) was developed to quantify the cumulative effect of pores on bone strength (Fig. 1*A*). Because whole-bone strength is related to the third power of bone width, the impact of individual pores on whole-bone strength depends on pore area (A_i) and the distance of the pore to the bending plane (d_i), which was calculated as the neutral axis based on standard beam theory. CPS_{plane} was assessed on an absolute basis and as a percentage of the moment of inertia calculated after all pores were filled ($I_{MLfilled}$). To test how CPS calculated relative to a bending plane (CPS_{plane}) correlated with CPS calculated without assuming a loading direction, we also calculated CPS_{point} where d_i was measured as the distance of each pore centroid to the geometric centroid of the bone cross-section, which was calculated relative to the thresholded cross-section, including marrow and pores. A validation study comparing the processed image with the original image for four bone regions (2-mm-wide swaths located along the *A*, *P*, *M*, and *L* axes and extending from the periosteal to the endocortical surfaces) from 3 donors revealed that our method led to false-positive and false-negative rates of 5.4% and 6.0%, respectively. The false-positive and false-negative pores were very small (~4 to 6 pixels in size) and near the threshold for minimum pore size. As such, our processing method affected pore number modestly, but because of the very small size of the

pores was expected to minimally affect measures of porosity and CPS.

Ash content

Sections used to assess ash content were defatted, weighed while submerged in distilled water (submerged weight), centrifuged at 8000*g* to remove adherent water and weighed in air (hydrated weight), dried to constant weight and weighed (dry weight), then ashed at 600°C and weighed (ash weight). Ash content was calculated as the ash weight/hydrated weight.[30]

Raman spectroscopy

Cross-sections were thawed, cleaned of marrow, and polished on silicon carbide paper. Raman spectra were acquired under hydrated conditions using a stainless-steel MultiRxn-immersion fiberoptic probe attached to a portable RamanRxn1 spectrometer equipped with a near-infrared laser (Invictus NIR laser 785 nm, 0.27 numerical aperture), a 256 × 1024 front illuminated CCD detector (cooled to -40°C), and an axial-transmissive spectrograph fitted with a 50 µm slit (± 4 cm^{-1} spectral resolution; Kaiser Optical Systems, Ann Arbor, MI, USA).[31] Midcortical spectra were acquired using the Andor Solis Software (Andor Technologies, Belfast, Northern Ireland) using 6 × 10 s acquisition times (laser spot size = ~100 µm, power output = ~87 mW). Duplicate spectral measurements were acquired from the lateral, medial, anterior, and posterior quadrants.

Spectroscopic data were processed and calibrated using custom written MATLAB scripts (The MathWorks, Natick, MA, USA). Spectra were imported into GRAMS/AI software (Thermo Fisher Scientific, Waltham, MA, USA) for spectral averaging, baseline correction, and normalization.[32] For curve-fitting, second derivative and constrained Gaussian deconvolution functions were applied to the following spectral regions: 802 to 894, 900 to 990, 1215 to 1360, and 1534 to 1721 cm^{-1}. Select band height ratios were used to calculate the following spectroscopic measures: mineral/matrix ratio (MMR; 960/853 cm^{-1}), hydroxyproline/proline ratio (hyp/pro ratio; 875/853 cm^{-1}), lipid/matrix ratio (1299/1340 cm^{-1}), collagen disorder/order

ratio (1246/1269 cm^{-1}), and collagen crosslinks ratio (Xlinks; 1665/1692 cm^{-1}). Collagen disorder/order ratio relates to the amount of ordered α-helical collagen conformations in bone, including collagen orientation.[33,34] Mineral crystallinity was calculated as the inverse of the full width at half maximum (1/FWHM) of the Gaussian-fitted ν_1PO_4 band at 960 cm^{-1}. All measurements were averaged to provide a mean value for each specimen.

Tissue-level mechanical testing

Rectangular beams (55-mm long, 5-mm wide, 2.5-mm thick) were successfully milled from the diaphyseal sections of 35 samples using a customized CNC (computer numerical controlled) router (Velox VR-1414 CNC; Velox CNC, Orange, CA, USA). Beams were machined from the midcortex, closer to the periosteal surface. The beams were loaded to failure at 0.05 mm/s in four-point bending while submerged in 37°C PBS with added calcium,[35] as described previously.[36] Load and deflection were converted to stress and strain using bending equations that take yielding into consideration.[36] Tissue-level mechanical properties, which included tissue-modulus, strength, postyield strain (PYS), and energy-to-failure, were averaged if more than one sample was machined from the radius. Tissue-level strength, which differs from whole-bone strength, refers to the maximum stress calculated for the beams.

Statistical analysis

Whole-bone mechanical properties of the male radii have been previously reported,[37] but are being examined herein in the context of subgroup analysis and biomechanical mechanisms that were not tested previously. Traits that failed the D'Agostino and Pearson Omnibus Normality Test were logarithm-transformed. First, a partial linear regression analysis was conducted between each porosity measure and robustness while accounting for age to test whether male radii showed associations between porosity and external bone size similar to previous studies.[17–20] Second, the data were sorted into narrow (n = 18) and wide (n = 19) subgroups using height-adjusted robustness, which is the residual calculated from a linear

regression between robustness and height. Only two subgroups were examined to maximize statistical power. The data were rank-ordered for height-adjusted robustness and the middle three samples of each subgroup were excluded from the statistical analysis to delineate the two subgroups on a practical and statistical basis. We excluded these samples because designating the middle samples as narrow or wide appeared somewhat arbitrary as it depended on the number of samples that were included in the study or whether the samples were rank ordered based on the absolute value of robustness rather than height-adjusted robustness. Linear regression analyses were conducted between all properties and age, and the slope and *y*-intercepts of the narrow and wide subgroups were compared using ANCOVA (GraphPad Prism v. 7.04; GraphPad Software, La Jolla, CA, USA). A sensitivity analysis was conducted by repeating the regression analyses with the data segregated into tertiles (comparing the narrow and wide tertiles) and by systematically excluding 0, 1, 2, or 3 rank-ordered samples from each subgroup.

A multivariate regression analysis was conducted to identify a set of traits that predicted whole-bone strength using the entire dataset (SPSS Statistics v. 24.0; IBM Corp., Armonk, NY, USA). The multivariate regression model was systematically reduced by eliminating traits that did not contribute significantly to whole-bone strength until the adjusted R^2 value was maximized and all variance inflation factors (VIFs) were below 5.[38] We used this systematic approach rather than a stepwise regression analysis because engineering principles provide a prescribed assemblage of factors that contribute to whole-bone strength (Fig. 1*B*) and the variable-reduction process provides insight into the relative importance of individual traits to whole-bone strength. The model was initiated by choosing morphological and material traits from among the three categories shown in Fig. 1*B*. Age and height were included in all models. Weight contributes significantly to bone morphology during growth, resulting in adults and subadults showing strong associations between weight and bone morphology.[39–41] However, weight was not considered a reliable adjustment factor for our analysis of bone strength across the lifespan because the weight reported at time of death is highly variable, depending on the nature and length of prior illness, and may not reflect the weight magnitude that defined bone

morphology and strength during growth. However, height remains relatively constant and more invariant to lifestyle changes and illness. As such, body-size adjustments included measures of bone length and body height. For whole-bone mechanical properties, PYD was included because reductions in PYD are associated with reduced strength.[37,42] For morphology, robustness and Ct.Ar were included instead of moment of inertia to allow us to break out specific aspects of the morphology (eg, external size, the amount of bone) to more systemically investigate why the strength–age regressions differ between the narrow and wide subgroups. Moment of inertia, although highly correlated with strength, is a more complicated morphological trait as it reflects both the external size of bone and the amount of bone, albeit in nonlinear ways (ie, external size is more heavily weighted in the calculation of moment of inertia than the amount of bone). For tissue-level mechanical properties, we included tissue-strength, porosity, MMR, and Xlinks ratio because these traits are thought to contribute to whole-bone strength. Alternate traits were substituted when one existed (eg, tissue-level PYS was substituted for whole-bone PYD, ash content was substituted for MMR, etc.) to test whether the multivariate regression outcomes (adjusted R^2, VIFs) were sensitive to omitted variables.

Results

Associations between porosity and external bone size

Donor ages and anthropometric traits are given in Table 1. A partial regression analysis was conducted to test whether porosity measures were associated with robustness while controlling for age (Table 2). Pearson correlation coefficients were significant ($p < 0.05$) or borderline significant ($p < 0.10$) for all porosity measures except pore density, indicating that narrow radii tended to have a lower overall porosity, lower midcortical porosity, smaller pore area, ans smaller CPS_{plane} and CPS_{point}, but no difference in pore density compared with wide radii. $Log(CPS_{plane})$ correlated significantly with $log(CPS_{point})$ ($R^2 = 0.981$, $p < 0.001$; data not shown), suggesting that calculating CPS without assuming a bending plane (CPS_{point}) was highly correlated with calculating CPS relative to the experimental bending plane used in this study

(CPS_{plane}).

Associations between external bone size and body size

Male radii showed a nonsignificant correlation between robustness and height (R^2 = 0.007, p = 0.611; data not shown), even when adjusting for age (R^2 = 0.014, p = 0.484). Rank ordering the samples without adjusting for height resulted in two samples that flipped from being designated as narrow versus wide. This outcome motivated the exclusion of the middle six samples for all regression analyses so the outcomes would be insensitive to the choice of body-size adjustment.

Whole-bone strength

Radii were loaded to failure in four-point bending to assess whole-bone strength (ie, maximum bending moment). A nonsignificant association was observed between whole-bone strength and age when all the data were included in a single regression (Fig. 2*A*). The data were sorted into narrow and wide subgroups using height-adjusted robustness. The average age (narrow: 45.2 ± 23.2 years; wide: 59.6 ± 21.9 years; p = 0.087), weight (narrow: 80.4 ± 20.7 kg; wide: 90.7 ± 33.6 kg; p = 0.317), BMI (narrow: 25.7 ± 6.0 kg/m^2; wide: 28.5 ± 9.9 kg/m^2; p = 0.354), and height (narrow: 1.77 ± 0.09 m; wide: 1.78 ± 0.10 m; p = 0.698) were not statistically different between subgroups (Student's t test). A significant negative correlation was observed between whole-bone strength and age for the wide but not the narrow subgroup (Fig. 2*B*). The slopes differed significantly between the subgroups (p = 0.017, ANCOVA), which was confirmed with a sensitivity analysis that varied the number of rank-ordered samples that were excluded from the analysis from zero to three per subgroup and when segregating the data into tertiles and comparing the most narrow and wide tertiles. Comparing strength values of young (< 40 years) and older males (> 65 years) between subgroups by two-way ANOVA showed significant effects because of age (p = 0.022), robustness (p < 0.0001), and the interaction between age and robustness (p = 0.005). The strength of young wide radii (70.31 ± 5.10 Nm, n = 5) was 54% greater (p < 0.0001, Tukey post hoc test) compared with young narrow radii (45.78

± 9.72 Nm, n = 8). In contrast, the strength of older wide radii (53.21 ± 3.15 Nm, n = 6) was not significantly different (p = 0.647, Tukey post hoc test) compared with older narrow radii (47.93 ± 5.72 Nm, n = 4).

Bone morphology

Midshaft morphological traits were assessed and plotted against age to compare the trait–age regressions that may imply different structural changes between the narrow and wide subgroups. Significant positive correlations were observed between age and robustness, Ct.Ar, and I_{ML} for the narrow but not the wide subgroup (Fig. 3). Ma.Ar did not correlate significantly with age for either subgroup. The slope or *y*-intercept of the linear regressions differed between the subgroups for each of the morphological traits shown in Fig. 3.

Porosity

Porosity measures were plotted against age and compared to determine if the amount and location of pores differed between the narrow and wide subgroups. Overall porosity and midcortical porosity correlated positively with age for the narrow and wide subgroups (Fig. 4*A*, *B*). Significant and borderline significant correlations were found between pore area and age for the narrow and wide subgroups, respectively (Fig. 4*C*). Neither subgroup showed a significant correlation between pore density and age (narrow: R^2 = 0.031, p = 0.531; wide R^2 = 0.039, p = 0.466; data not shown). The regression between log(CPS_{plane}) and log(overall porosity) differed significantly between narrow and wide subgroups (Fig. 4*D*), indicating that CPS_{plane} was significantly greater for a given porosity in wide compared with narrow radii, as expected. A significant positive correlation was found between log(CPS_{plane}) and age for the narrow but not the wide subgroups (Fig. 4*E*), with the wide subgroup showing a significantly greater *y*-intercept compared with the narrow subgroup. This was confirmed when CPS_{plane} was expressed as a percentage of $I_{MLfilled}$, which is the moment of inertia relative to the applied bending loads calculated with all pores filled (Fig. 4*F*). CPS_{plane} accounted for 2.7% to 9.5% of I_{ML} for the

elderly narrow subgroup and 5.0% to 25.5% of $I_{MLfilled}$ for the elderly wide subgroup (data not shown).

Matrix composition

Raman spectroscopic measures were plotted against age and compared to determine if matrix composition differed between the narrow and wide subgroups. Linear regression analysis showed significant correlations with age for log(collagen disorder/order ratio) and lipid/matrix ratio for both subgroups (Fig. 5*A*, *B*). Significant positive associations between MMR and log(hyp/pro ratio) and age were found for the narrow but not the wide subgroup (Fig. 5*C*, *D*). A significant correlation between ash content and age for the narrow (R^2 = 0.355, p = 0.019) but not wide (R^2 = 0.026, p = 0.567) subgroups (data not shown) confirmed the MMR outcomes. A significant negative correlation was found between log(Xlinks ratio) and age for the wide but not the narrow subgroup (Fig. 5*E*). Finally, mineral crystallinity did not correlate significantly with age for either subgroup (Fig. 5*F*).

Tissue-level mechanical properties

Tissue-level mechanical properties were assessed for all samples and the linear regressions were compared to test whether the wide subgroup would show a significantly greater decline in the strength-age regression compared with the narrow subgroup, similar to that observed at the whole-bone level. Tissue stiffness (modulus) did not show a significant correlation with age for either subgroup (Fig. 6). However, tissue strength and energy-to-failure showed significant negative correlations with age for the wide but not the narrow subgroup. A significant negative correlation was found between tissue PYS and age for both subgroups.

Multivariate regression analysis

A multivariate regression analysis was conducted to identify the significant predictors of whole-bone strength. The initial group of traits predicted whole-bone strength with an adjusted

R^2 of 0.768 ($p < 0.0001$; model 1, Table 3), but several VIFs exceeded 5. Replacing height with either weight or BMI resulted in both terms being eliminated in the first round as neither were significant predictors of strength. Systematically eliminating traits with nonsignificant contributions resulted in a model with age, height, robustness, porosity, and MMR (model 5, adj. $R^2 = 0.803$, $p < 0.0001$) and VIF below 2.7. Replacing MMR and porosity with Ct.TMD (model 6), which can be assessed noninvasively, improved the model (adj. $R^2 = 0.907$, $p < 0.0001$) with all VIFs below 1.6. The sensitivity of the model to the choice of traits was tested by replacing traits (eg, PYS for PYD, ash for MMR) or including omitted traits (eg, lipid/matrix ratio). This analysis resulted in models with similar adjusted R^2 values, but with slightly different components (data not shown). In general, the models included measures of external bone size, porosity, and mineralization in addition to age and height.

Discussion

The results of this study support the hypothesis that wide radii would show a more negative correlation between whole-bone strength and age compared with narrow radii (Fig. 2*B*). Male radii were sorted into narrow and wide subgroups using height-adjusted robustness to minimize body-size effects, consistent with our prior work.[18] The 54% greater strength of young adult wide radii compared with narrow radii was expected and is thought to result from limitations in the adaptive process that occurs during bone growth.[18,26,43,44] This strength gradient may help explain why young adults with increased fracture risk tend to have narrow bones.[45–48] Importantly, the greater strength of young adult wide radii was lost with age, as both subgroups converged toward similar strength values after 65 years of age. Thus, the low strength of elderly male radii arose through different strength-decline trajectories: The narrow radii showed low strength for young adults was maintained with age, whereas the wide radii showed high strength for young adults, much of which was lost with age. Whole bone strength of elderly individuals varies with many factors such as sex,[49–52] ethnicity/race,[53] weight loss and frailty,[54] and rates of bone loss.[55] The current study provided evidence that external bone size also affects the

strength of elderly male radii by influencing bone strength-decline trajectories.

The biomechanical mechanisms that define how structural and material changes contributed to the different strength-decline trajectories (Fig. 7) were constructed based on the outcomes of the trait–age regressions (Figs. 3 through 6) and the multivariate regression analysis (Table 3), and contextualized with known associations among physical traits and whole-bone strength.[28] The nonsignificant correlation between strength and age for the narrow subgroup appeared to result from increases in robustness, Ct.Ar, and mineralization (MMR) that mechanically offset increases in porosity. Thus, it appeared that external size and composition were adjusted to maintain strength in narrow radii across the age range examined. In contrast, the negative correlation between strength and age for wide radii appeared to occur because external size did not increase to mechanically offset increases in porosity and reductions in tissue strength. Thus, differences in the amount of periosteal expansion appeared to be a critical factor explaining the different strength-decline trajectories of the narrow and wide subgroups. Although the strength-decline trajectories were limited to data derived from cadaveric tissue, the different robustness–age regressions observed for the male radii were consistent with those reported for the femoral neck based on an analysis of longitudinal data for women[15] and men[16]. This outcome suggested that there are biological factors that stimulate periosteal expansion in narrow bones, but either suppress or fail to stimulate periosteal expansion in wide bones.

Periosteal expansion is a critical structural change that helps maintain bone strength with aging,[56–58] and is generally thought to be stimulated by bone loss, which occurs in the form of increased porosity for long bone diaphyses.[23] However, the distance of pores to the geometric centroid may also affect how age-related increases in pore size affect whole-bone strength. This effect was captured by a new measure called the Cortical Pore Score, which we developed to assess the cumulative impact of individual pore sizes and their location on bone strength. To maintain strength with aging, wide bones theoretically need to show a greater amount of periosteal expansion compared with narrow bones because the large, subendocortical pores associated with age-related bone loss[23,29] are located proportionally further from the geometric

centroid.[59] However, the opposite was found for the male radii: The wide subgroup showed a nonsignificant association between robustness and age, whereas the narrow subgroup showed a significant positive association (Fig. 3). Neither the amount nor the location of pores explained the differences in periosteal expansion between the narrow and wide subgroups. First, wide radii tended to have larger pores compared with narrow radii (Table 2), consistent with previous work.[17–20] Second, the two subgroups did not show different associations between porosity and age (Fig. 4), suggesting that the greater baseline porosity of wide bones did not confer greater age-related bone loss in the male radius. The age-related increase in porosity resulted from an increase in pore size, but not pore density, for both subgroups, consistent with work by others.[60,61] The similar porosity–age regressions for the subgroups contradicted prior work, including our own, showing that bone width is positively associated with measures of resorption.[15,16,19,21] Additional research is needed to understand how the association between remodeling and external size varies with anatomical site, sex, and age. Third, the age-related increase in porosity accounted for a greater fraction of the moment of inertia in wide bones (Fig 4*F*), confirming that the greater distance of the pores to the geometric centroid exacerbated the deleterious effects of porosity on strength. The greater CPS of wide radii may have contributed to the strength decline, but did not appear to stimulate periosteal expansion to offset bone loss. Thus, our subgroup analysis indicated that periosteal expansion may not be simply coupled to bone loss, as is generally thought.[21,62]

Whole-bone strength is also influenced by tissue-level mechanical properties, which are defined by tissue composition and porosity. This was confirmed in the multivariate regression analysis. Tissue strength decreased with age in the wide but not narrow subgroup, although both subgroups showed similar declines in postyield strain. Raman spectroscopy identified compositional traits that showed similar correlations with age for both subgroups (mineral crystallinity, collagen disorder/order ratio, and lipid/matrix ratio) and traits that showed positive (MMR, hyp/pro ratio) or negative (Xlinks ratio) correlations with age in only one subgroup. The significant positive correlation between MMR and age for the narrow subgroup (Fig. 5) was

consistent with the slightly lower midcortex porosity measures for the narrow subgroup (Fig. 4*B*), which may indicate a lower amount of remodeling in the region where Raman spectroscopy was conducted. In general, bone with low remodeling activity retains more complete mineralization of secondary bone.[63] Thus, the age-related increase in mineralization in narrow bones appears to have offset the increase in overall porosity, resulting in similar tissue-strength values across the age range examined for this subgroup. The dependence of bone strength on collagen crosslink content,[64] porosity,[65] and mineralization [65] could explain why whole-bone strength declined with age for the wide subgroup. The contribution of additional matrix (eg, advanced glycation endproducts) and microarchitectural parameters (eg, osteon size) on bone strength can be examined in future work.

There are several clinical implications of the data that are worth noting. The lack of differences in strength between the narrow and wide subgroups for elderly males may help explain inconsistencies among studies reporting that individuals with fractures range from having more narrow bones[66,67] to wider bones[19,68–71] compared with nonfracture cohorts. Although further investigations are needed to better understand individual strength-decline trajectories and how they relate to fracture incidence, the concept that strength-decline trajectories differ among individuals could make it difficult to identify a single trait or a single combination of traits that predicts fracture risk across a population. The specific morphological and material changes underlying the different strength–age trajectories may provide targets for these treatment strategies. For example, treatments that suppress remodeling may benefit individuals with wide bones given that the further location of the pores from the geometric centroid may exacerbate the deleterious effects of porosity on strength. We stratified our donor samples into two subgroups based on height-adjusted robustness, not an underlying disease or fragility fracture status. We suspect that other factors that are known to influence bone strength and morphology within a single sex and ethnicity such as disease, weight change, estrogen replacement therapy use,[72] and hormone levels[73] may be superimposed on this underlying morphological effect and would contribute to the variation in strength within each subgroup. We

were not able to test for these additional factors given the limited life-history information of the donors. Studying strength changes using longitudinal databases would be needed to refine these additional effects and to test for interactions with baseline external bone size.

The biomechanical mechanisms derived from this study are limited to how well trait–age regressions of cadaveric tissue reflect longitudinal changes in bone. As previously noted, the robustness–age regressions observed in the current study were consistent with those from longitudinal studies of the femoral neck,[15,16] suggesting that the biomechanical mechanisms derived herein may provide important clues to interindividual differences in skeletal aging. The current study was limited to the radial diaphysis of white males, and it is unclear if similar strength–age trajectories and biomechanical mechanisms will be observed for other skeletal sites, women, or other ethnicities. Finally, the current study was powered to test for differences in strength–age regressions, which may have limited the power to detect significant differences in porosity. There was sufficient power to detect statistical differences among the primary outcome variables like strength, robustness, cortical area, and most of the tissue-level traits. However, a couple of the porosity variables showed borderline differences in *y*-intercepts between the narrow and wide subgroups (eg, midcortical porosity, $CPS_{plane}/I_{MLfilled}$). For these variables, a power analysis using a significance level of 0.05 and power of 0.8 confirmed that confirmed sample sizes of 18 to 25 would be needed to detect significant differences between regressions for the narrow and wide subgroups.[74] Thus, our study was appropriately powered for whole-bone strength but not for all of the porosity variables.

In conclusion, our study showed that elderly white male radii arrived at similar low strength values through fundamentally different biomechanical mechanisms. This outcome provided evidence that more than one strength-decline trajectory exists within a single sex and ethnicity. The different biomechanical mechanisms illustrated in Fig. 7 argue that the associations between strength and morphology will vary among elderly individuals depending on their baseline external bone size and strength-decline trajectory,[53] and that fracture-outcome studies may benefit from testing for multiple biomechanical pathways leading to fracture risk.[48]

Disclosures

The authors have no conflicts of interest to declare.

Acknowledgments

Research reported in this publication was supported by the National Institute of Arthritis and Musculoskeletal and Skin Diseases of the National Institutes of Health (KJJ: AR065424, AR069620, AR068452; SHS: AR070903; DHK: T32DE007057; TLB: AR064244). The content is solely the responsibility of the authors and does not necessarily represent the official views of the National Institutes of Health.

Authors' roles:[0]

References

1. Hayes WC, Myers ER, Robinovitch SN, Van Den Kroonenberg A, Courtney AC, McMahon TA. Etiology and prevention of age-related hip fractures. Bone. 1996;18(1 Suppl):77S–86S.

2. Johnell O, Kanis JA. An estimate of the worldwide prevalence and disability associated with osteoporotic fractures. Osteoporos Int. 2006;17(12):1726–33.

3. Dyer SM, Crotty M, Fairhall N, et al. A critical review of the long-term disability outcomes following hip fracture. BMC Geriatr. 2016;16:158.

4. Burge R, Dawson-Hughes B, Solomon DH, Wong JB, King A, Tosteson A. Incidence and economic burden of osteoporosis-related fractures in the United States, 2005–2025. J Bone Miner Res. 2007;22(3):465–75.

5. Albright F, Smith PH, Richardson AM. Post-menopausal osteoporosis. Its clinical features. JAMA. 1941;116:2465–74.

6. Szulc P, Seeman E, Duboeuf F, Sornay-Rendu E, Delmas PD. Bone fragility: failure of periosteal apposition to compensate for increased endocortical resorption in postmenopausal women. J Bone Miner Res. 2006;21(12):1856–63.

7. Zebaze RM, Jones A, Knackstedt M, Maalouf G, Seeman E. Construction of the femoral neck during growth determines its strength in old age. J Bone Miner Res. 2007;22(7):1055–61.

8. Vashishth D. The role of the collagen matrix in skeletal fragility. Curr Osteoporos Rep. 2007;5(2):62–6.

9. Karlsson MK, Ahlborg HG, Svejme O, Nilsson JA, Rosengren BE. An increase in forearm cortical bone size after menopause may influence the estimated bone mineral loss–a 28-year prospective observational study. J Clin Densitom. 2016 Apr–Jun;19(2):174–9.

10. Wang XF, Duan Y, Beck TJ, Seeman E. Varying contributions of growth and ageing to racial and sex differences in femoral neck structure and strength in old age. Bone. 2005;36(6):978–86.

11. Russo CR, Lauretani F, Seeman E, et al. Structural adaptations to bone loss in aging men and women. Bone. 2006;38(1):112–8.

12. Travison TG, Beck TJ, Esche GR, Araujo AB, McKinlay JB. Age trends in proximal femur geometry in men: variation by race and ethnicity. Osteoporos Int. 2008;19(3):277–87.

13. Christiansen BA, Kopperdahl DL, Kiel DP, Keaveny TM, Bouxsein ML. Mechanical contributions of the cortical and trabecular compartments contribute to differences in age-related changes in vertebral body strength in men and women assessed by QCT-based finite element analysis. J Bone Miner Res. 2011;26(5):974–83.

14. Djonic D, Milovanovic P, Nikolic S, et al. Inter-sex differences in structural properties of aging femora: implications on differential bone fragility: a cadaver study. J Bone Miner Metab. 2011;29(4):449–57.

15. Jepsen KJ, Kozminski A, Bigelow EM, et al. Femoral neck external size but not aBMD predicts structural and mass changes for women transitioning through menopause. J Bone Miner Res. 2017;32(6):1218–28.

16. Cawthon PM, Ewing SK, McCulloch CE, et al. Loss of hip BMD in older men: the osteoporotic fractures in men (MrOS) study. J Bone Miner Res. 2009;24(10):1728–35.

17. Ural A, Vashishth D. Interactions between microstructural and geometrical adaptation in human cortical bone. J Orthop Res. 2006;24(7):1489–98.

18. Jepsen KJ, Centi A, Duarte GF, et al. Biological constraints that limit compensation of a common skeletal trait variant lead to inequivalence of tibial function among healthy young adults. J Bone Miner Res. 2011;26(12):2872–5.

19. Bjornerem A, Bui QM, Ghasem-Zadeh A, Hopper JL, Zebaze R, Seeman E. Fracture risk and height: an association partly accounted for by cortical porosity of relatively thinner cortices. J Bone Miner Res. 2013;28(9):2017–26.

20. Goldman HM, Hampson NA, Guth JJ, Lin D, Jepsen KJ. Intracortical remodeling parameters are associated with measures of bone robustness. Anat Rec (Hoboken). 2014;297(10):1817–28.

21. Kemp JP, Sayers A, Paternoster L, et al. Does bone resorption stimulate periosteal expansion? A cross-sectional analysis of beta-C-telopeptides of type I collagen (CTX), genetic markers of the RANKL pathway, and periosteal circumference as measured by pQCT. J Bone Miner Res. 2014;29(4):1015–24.

22. Parfitt AM. Age-related structural changes in trabecular and cortical bone: cellular mechanisms and biomechanical consequences. Calc Tissue Int. 1984;36(Suppl 1):S123–8.

23. Zebaze RM, Ghasem-Zadeh A, Bohte A, I et al. Intracortical remodelling and porosity in the distal radius and post-mortem femurs of women: a cross-sectional study. Lancet. 2010;375(9727):1729–36.

24. Auerbach BM, Ruff CB. Limb bone bilateral asymmetry: variability and commonality among modern humans. J Hum Evol. 2006;50(2):203–18.

25. Schneider CA, Rasband WS, Eliceiri KW. NIH Image to ImageJ: 25 years of image analysis. Nat Methods. 2012;9(7):671–5.

26. Schlecht SH, Bigelow EM, Jepsen KJ. Mapping the natural variation in whole bone stiffness and strength across skeletal sites. Bone. 2014;67:15–22.

27. Frush DP DL, Rosen NS. Computed tomography and radiation risks: what pediatric health care providers should know. Pediatrics. 2003;112(4):951–7.

28. Jepsen KJ, Silva MJ, Vashishth D, Guo XE, van der Meulen M. Establishing biomechanical mechanisms in mouse models: practical guidelines for systematically evaluating phenotypic changes in the diaphyses of long bones. J Bone Miner Res. 2015;30(6):951–66.

29. Andreasen CM, Delaisse JM, Cj van der Eerden B, van Leeuwen JP, Ding M, Andersen TL. Understanding age-induced cortical porosity in women: the accumulation and coalescence of eroded cavities upon existing intracortical canals is the main contributor. J Bone Miner Res. 2017;33(4):606–20.

30. Tommasini SM, Nasser P, Hu B, Jepsen KJ. Biological co-adaptation of morphological and composition traits contributes to mechanical functionality and skeletal fragility. J Bone Miner Res. 2008;23(2):236–46.

31. Peterson JR, Okagbare PI, De La Rosa S, et al. Early detection of burn induced heterotopic ossification using transcutaneous Raman spectroscopy. Bone. 2013;54(1):28–34.

32. Shi C, Mandair GS, Zhang H, et al. Bone morphogenetic protein signaling through ACVR1 and BMPR1A negatively regulates bone mass along with alterations in bone composition. Journal of structural biology. 2018;201(3):237–46.

33. Mandair GS, Morris MD. Contributions of Raman spectroscopy to the understanding of bone strength. Bonekey Rep. 2015;4:620.

34. Unal M, Jung H, Akkus O. Novel raman spectroscopic biomarkers indicate that postyield damage denatures bone's collagen. J Bone Miner Res. 2016;31(5):1015–25.

35. Gustafson MB, Martin RB, Gibson V, et al. Calcium buffering is required to maintain bone stiffness in saline solution. J Biomech. 1996;29(9):1191–4.

36. Tommasini SM, Nasser P, Schaffler MB, Jepsen KJ. Relationship between bone morphology and bone quality in male tibias: implications for stress fracture risk. J Bone Miner Res. 2005;20(8):1372–80.

37. Patton DM, Bigelow EM, Schlecht SH, Kohn D, Bredbenner TL, Jepson JK. The relationship between whole bone stiffness and strength is age and sex dependent. J Biomech. 2019 Jan 23;83:125–133.

38. Stine RA. Graphical interpretation of variance inflation factors. Amer Statist. 1995;49(1):53–6.

39. Moro M, van der Meulen MC, Kiratli BJ, Marcus R, Bachrach LK, Carter DR. Body mass is the primary determinant of midfemoral bone acquisition during adolescent growth. Bone. 1996;19(5):519–26.

40. Ruff C. Growth in bone strength, body size, and muscle size in a juvenile longitudinal sample. Bone. 2003;33(3):317–29.

41. Ruff C. Growth tracking of femoral and humeral strength from infancy through late adolescence. Acta Paediatr. 2005;94(8):1030–7.

42. Nawathe S, Yang H, Fields AJ, Bouxsein ML, Keaveny TM. Theoretical effects of fully ductile versus fully brittle behaviors of bone tissue on the strength of the human proximal femur and vertebral body. J Biomech. 2015;48(7):1264–9.

43. Jepsen KJ, Hu B, Tommasini SM, et al. Genetic randomization reveals functional relationships among morphologic and tissue-quality traits that contribute to bone strength and fragility. Mamm Genome. 2007;18(6–7):492–507.

44. Jepsen KJ, Hu B, Tommasini SM, et al. Phenotypic integration of skeletal traits during growth buffers genetic variants affecting the slenderness of femora in inbred mouse strains. Mamm Genome. 2009;20(1):21–33.

45. Milgrom C, Giladi M, Simkin A, et al. The area moment of inertia of the tibia: a risk factor for stress fractures. J Biomech. 1989;22(11–12):1243–8.

46. Crossley K, Bennell KL, Wrigley T, Oakes BW. Ground reaction forces, bone characteristics, and tibial stress fracture in male runners. Med Sci Sports Exerc. 1999;31(8):1088–93.

47. Beck TJ, Ruff CB, Shaffer RA, Betsinger K, Trone DW, Brodine SK. Stress fracture in military recruits: gender differences in muscle and bone susceptibility factors. Bone. 2000;27(3):437–44.

48. Jepsen KJ, Evans R, Negus C, et al. Variation in tibial functionality and fracture susceptibility among healthy, young adults arises from the acquisition of biologically distinct sets of traits. J Bone Miner Res. 2013;28(6):1290–300.

49. Beck TJ, Ruff CB, Scott WW, Plato CC, Tobin JD, Quan CA. Sex differences in geometry of the femoral neck with aging: a structural analysis of bone mineral data. Calcif Tissue Int. 1992;50(1):24–9.

50. Beck TJ, Looker AC, Ruff CB, Sievanen H, Wahner HW. Structural trends in the aging femoral neck and proximal shaft: analysis of the Third National Health and Nutrition Examination Survey dual-energy X-ray absorptiometry data. J Bone Miner Res. 2000;15(12):2297–304.

51. Looker AC, Beck TJ, Orwoll ES. Does body size account for gender differences in femur bone density and geometry? J Bone Miner Res. 2001;16(7):1291–9.

52. Duan Y, Beck TJ, Wang XF, Seeman E. Structural and biomechanical basis of sexual dimorphism in femoral neck fragility has its origins in growth and aging. J Bone Miner Res. 2003;18(10):1766–74.

53. Ishii S, Cauley JA, Greendale GA, et al. Trajectories of femoral neck strength in relation to the final menstrual period in a multi-ethnic cohort. Osteopor Int. 2013;24(9):2471–81.

54. Liu CT, Sahni S, Xu H, McLean RR, Broe KE, Hannan MT, et al. Long-term and recent weight change are associated with reduced peripheral bone eensity, deficits in bone microarchitecture, and decreased bone strength: the Framingham Osteoporosis Study. J Bone Miner Res. 2018.

55. Cauley JA, Burghardt AJ, Harrison SL, et al. Accelerated bone loss in older men: effects on bone microarchitecture and strength. J Bone Miner Res. Oct;33(10):1859–69.

56. Smith RW, Walker RR. Femoral expansion in aging women: Implications for osteoporosis and fractures. Science. 1964;145:156–7.

57. Ruff CB, Hayes WC. Subperiosteal expansion and cortical remodeling of the human femur and tibia with aging. Science. 1982;217:945–7.

58. Seeman E. Periosteal bone formation—a neglected determinant of bone strength. N Engl J Med. 2003;349(4):320–3.

59. Jepsen KJ, Andarawis-Puri N. The amount of periosteal apposition required to maintain bone strength during aging depends on adult bone morphology and tissue-modulus degradation rate. J Bone Miner Res. 2012;27(9):1916–26.

60. Thomas CD, Feik SA, Clement JG. Increase in pore area, and not pore density, is the main determinant in the development of porosity in human cortical bone. J Anat. 2006;209(2):219–30.

61. Cooper DM, Thomas CD, Clement JG, Turinsky AL, Sensen CW, Hallgrimsson B. Age-dependent change in the 3D structure of cortical porosity at the human femoral midshaft. Bone. 2007;40(4):957–65.

62. Seeman E. The periosteum—a surface for all seasons. Osteoporos Int. 2007;18(2):123–8.

63. Boivin G, Farlay D, Bala Y, Doublier A, Meunier PJ, Delmas PD. Influence of remodeling on the mineralization of bone tissue. Osteoporos Int. 2009;20(6):1023–6.

64. Garnero P. The contribution of collagen crosslinks to bone strength. Bonekey Rep. 2012;1:182.

65. Currey JD. The effect of porosity and mineral content on the Young's modulus of elasticity of compact bone. J Biomech. 1988;21(2):131–9.

66. Karlamangla AS, Barrett-Connor E, Young J, Greendale GA. Hip fracture risk assessment using composite indices of femoral neck strength: the Rancho Bernardo study. Osteoporos Int. 2004;15(1):62–70.

67. Szulc P, Munoz F, Duboeuf F, Marchand F, Delmas PD. Low width of tubular bones is associated with increased risk of fragility fracture in elderly men—the MINOS study. Bone. 2006;38(4):595–602.

68. Duan Y, Wang XF, Evans A, Seeman E. Structural and biomechanical basis of racial and sex differences in vertebral fragility in Chinese and Caucasians. Bone. 2005;36(6):987–98.

69. Kaptoge S, Beck TJ, Reeve J, et al. Prediction of incident hip fracture risk by femur geometry variables measured by hip structural analysis in the study of osteoporotic fractures. J Bone Miner Res. 2008;23(12):1892–904.

70. Shigdel R, Osima M, Ahmed LA, et al. Bone turnover markers are associated with higher cortical porosity, thinner cortices, and larger size of the proximal femur and non-vertebral fractures. Bone. 2015;81:1–6.

71. Leslie WD, Lix LM, Majumdar SR, et al. Total hip bone area affects fracture prediction with FRAX(R) in Canadian white women. J Clin Endocrinol Metab. 2017;102(11):4242–9.

72. Beck TJ, Stone KL, Oreskovic TL, et al. Effects of current and discontinued estrogen replacement therapy on hip structural geometry: the study of osteoporotic fractures. J Bone Miner Res. 2001;16(11):2103–10.

73. Ahlborg HG, Johnell O, Turner CH, Rannevik G, Karlsson MK. Bone loss and bone size after menopause. N Engl J Med. 2003;349(4):327–34.

74. Borm GF, Fransen J, Lemmens WA. A simple sample size formula for analysis of covariance in randomized clinical trials. J Clin Epidemiol. 2007;60(12):1234–8.

Fig. 1. (*A*) Schematic illustrating the two ways that the Cortical Pore Score was calculated from the nanoCT images (left: CPS_{plane}, right: CPS_{point}). Inset illustrates how voids adjacent to the marrow space were manually closed so they were included in the porosity analysis (arrows). (*B*) The flow chart shows known associations between physical bone traits and whole-bone strength. These associations helped inform decisions on the selection of traits used in the multivariate regression analysis and for establishing the biomechanical pathways responsible for different strength-decline trajectories. The flow chart shows three trait categories that contribute to bone strength. These include whole-bone mechanical properties, morphology, and tissue-level mechanical properties. The wide borders indicate the traits used in the multivariate regression analysis.

Fig. **2.** (*A*) A nonsignificant association was found between maximum bending moment (whole-bone strength) and age when all the data were included in a single regression. (*B*) Sorting the data based on height-adjusted robustness (excluding middle 3 rank-ordered subjects per subgroup) showed a significant association for wide but not narrow radii and a significant difference between the slopes of the two regressions (ANCOVA).

Fig. **3.** Linear regressions between (*A*) robustness, (*B*) cortical area, (*C*) marrow area, (*D*) moment of inertia (I_{ML}) and age differed between the narrow and wide subgroups.

Fig. **4.** Linear regressions between (*A*) overall porosity and age, (*B*) midcortical porosity and age, (*C*) average pore area and age, (*D*) CPS_{plane} and overall porosity, (*E*) CPS_{plane} and age, and (*F*) $CPS_{plane}/I_{MLfilled}$ and age for the narrow and wide subgroups.

Fig. **5.** Linear regressions between (*A*) collagen disorder/order ratio, (*B*) lipid/matrix ratio, (*C*) mineral/matrix ratio (MMR), (*D*) hydroxyproline/proline (hyp/pro) ratio, (*E*) collagen crosslinks (Xlinks) ratio, and (*F*) mineral crystallinity and age for the narrow and wide subgroups.

Fig. **6.** Linear regressions between (*A*) tissue-modulus, (*B*) tissue-strength, (*C*) tissue postyield

strain, (*D*) tissue energy-to-failure and age for the narrow and wide subgroups.

Fig. **7.** Schematic illustrating the different structural and material changes contributing to the biomechanical mechanisms that help explain the different strength–age regressions between narrow and wide subgroups.

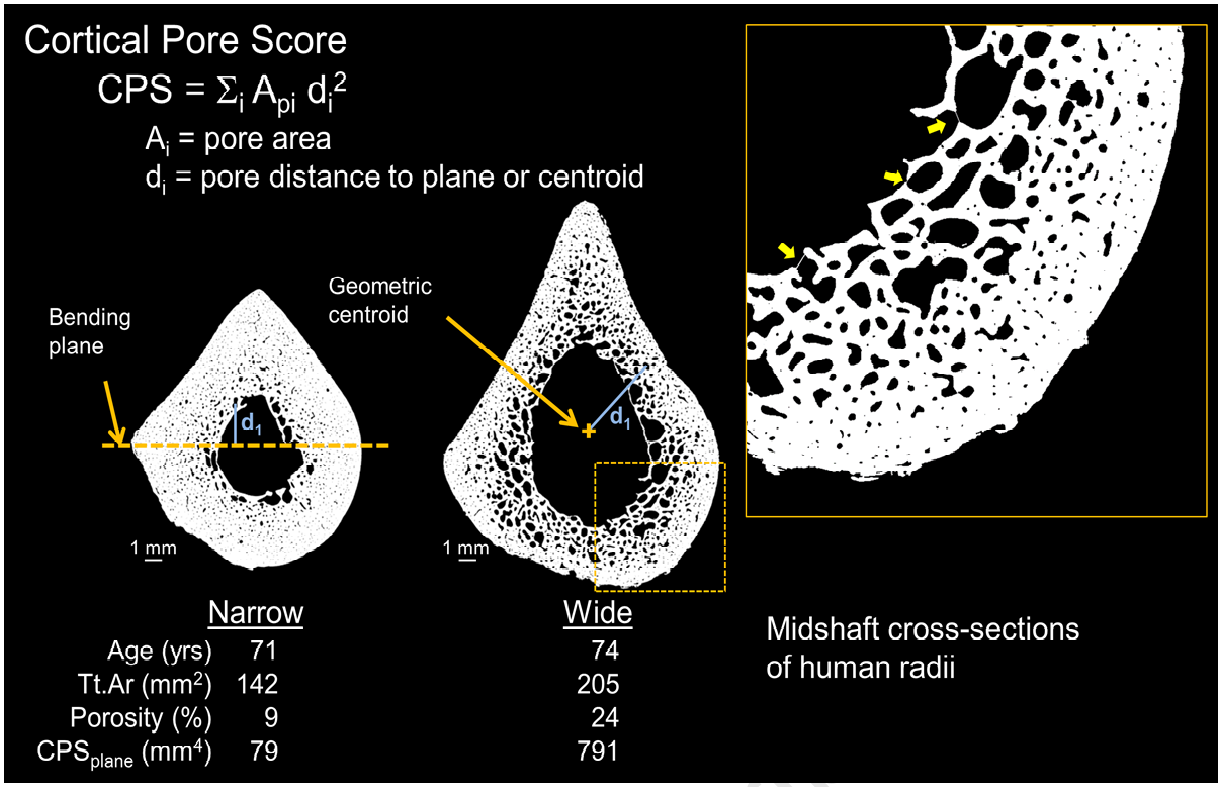

jbmr_3661_fig1A .

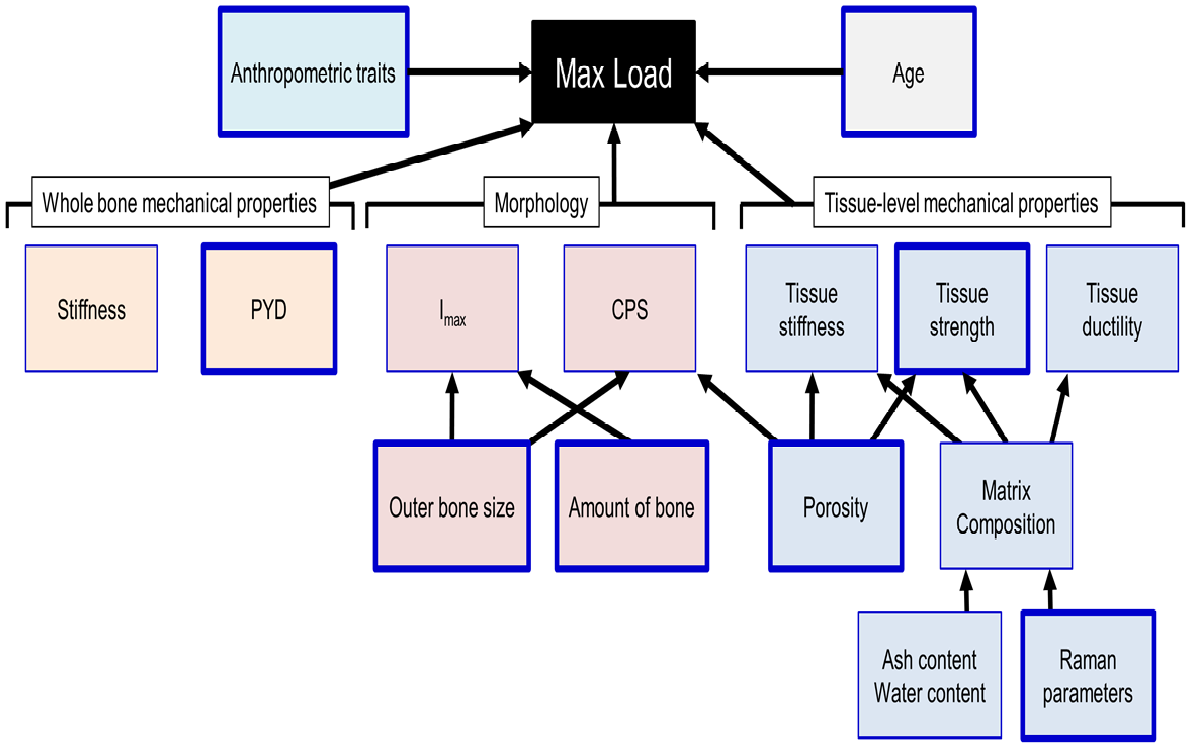

jbmr_3661_fig1B .

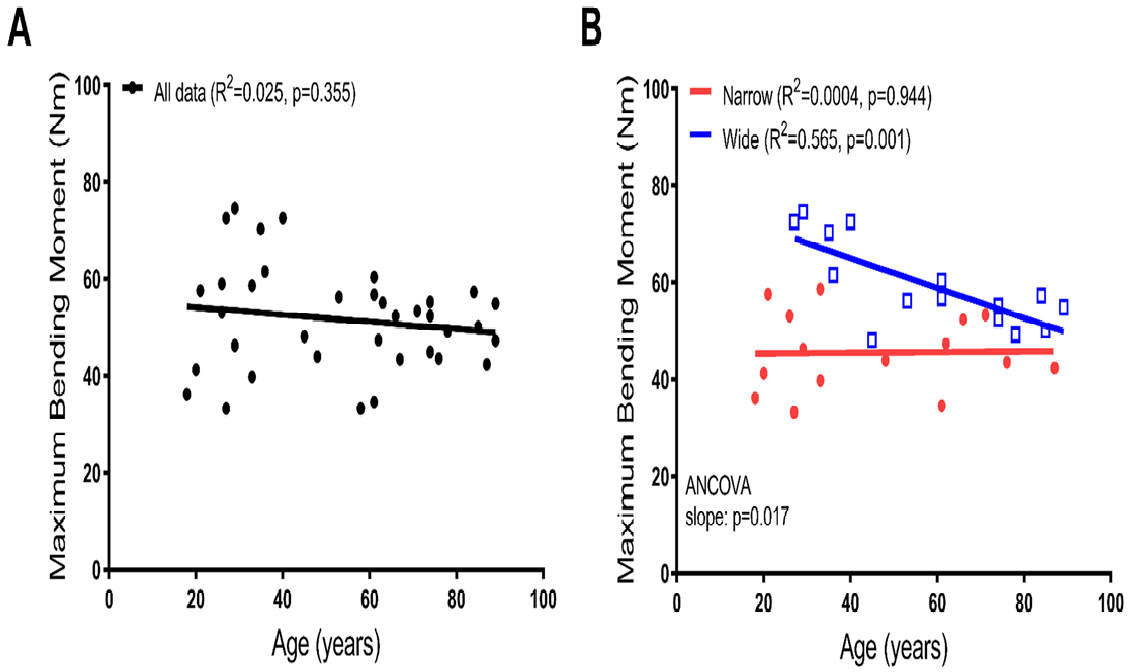

jbmr_3661_fig2 .

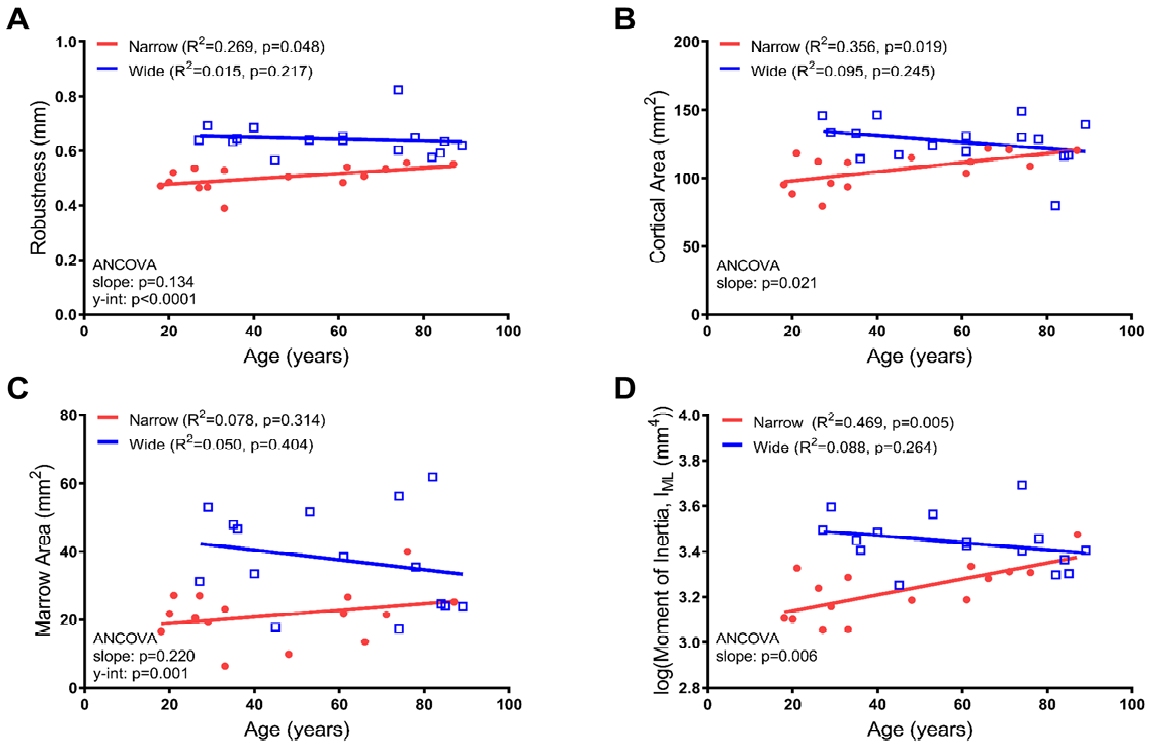

jbmr_3661_fig3 .

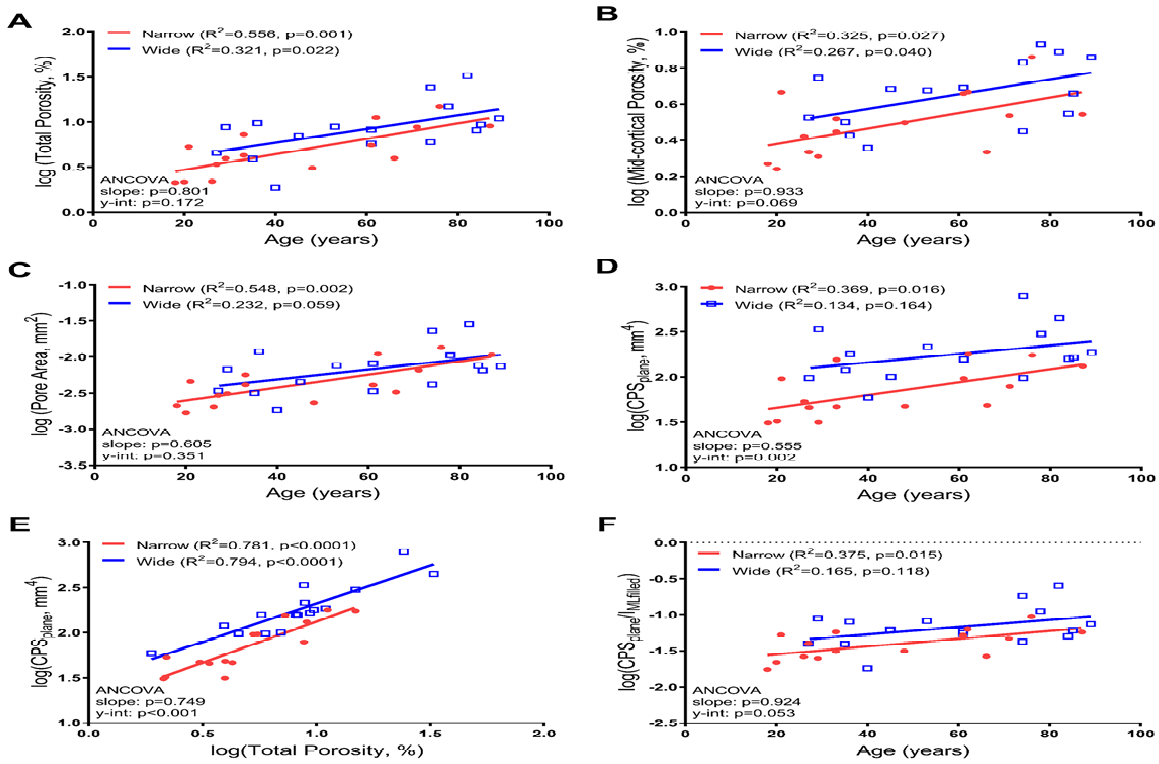

jbmr_3661_fig4 .

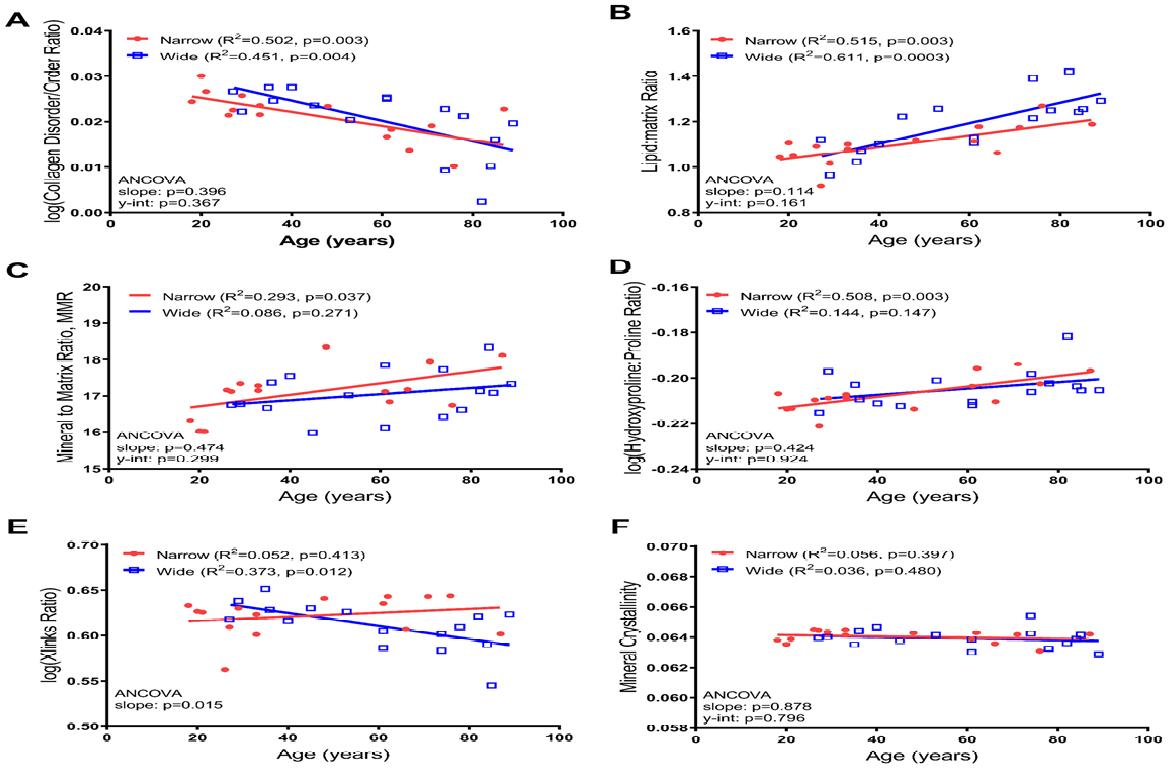

jbmr_3661_fig5 .

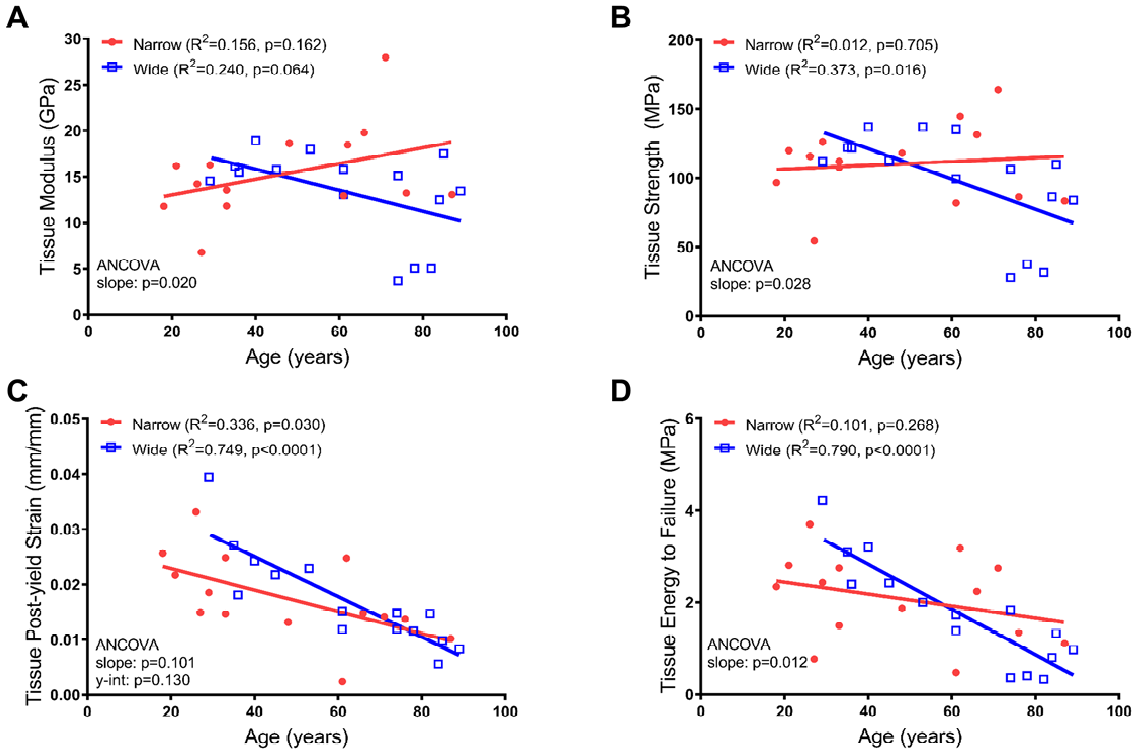

jbmr_3661_fig6 .

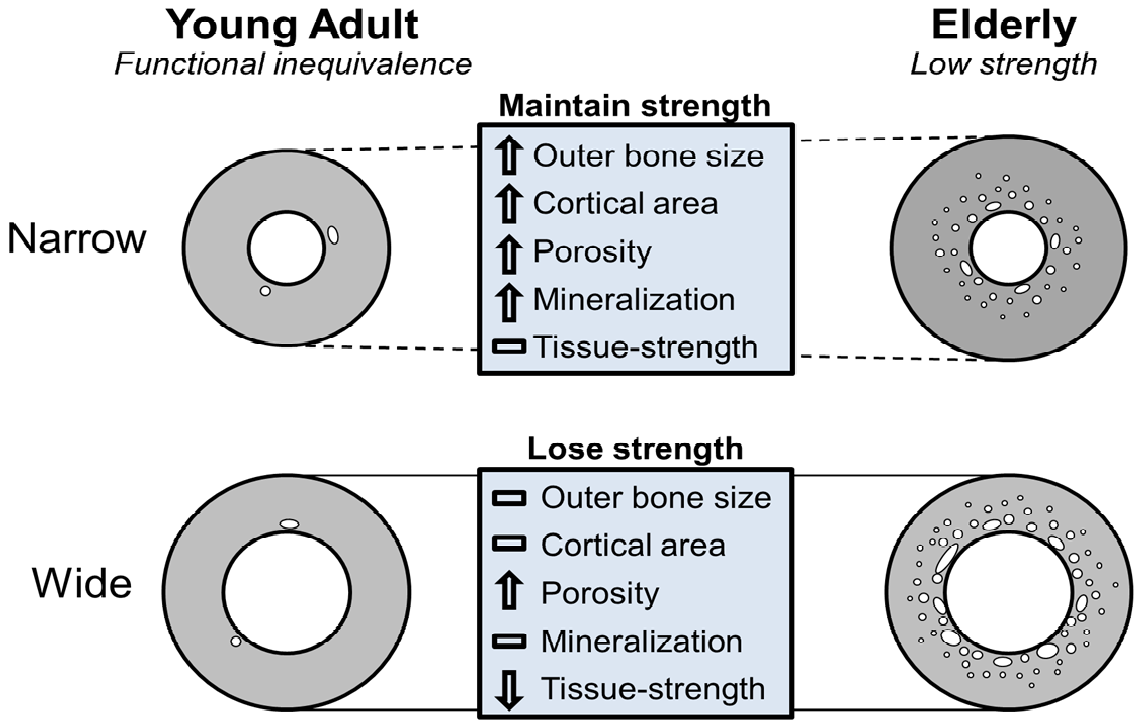

jbmr_3661_fig7 .